Supporting Information

Cu_2O/ZnO *p-n* junction decorated with NiO_x as protective layer and co-catalyst for enhanced photoelectrochemical water splitting

Jingxin Jian,[a] Raj Kumar,[b] and Jianwu Sun[*,a]*

[a]*Department of Physics, Chemistry and Biology (IFM), Linköping University, SE-58183, Linköping, Sweden.*

[b]*Department of Physics, Centre for Materials Science and Nanotechnology, Faculty of Mathematical and Natural Sciences, University of Oslo, P. O. Box 1048, Binden, 0316 Oslo, Norway.*

[*]*Corresponding author Jianwu Sun, E-mail: jianwu.sun@liu.se*

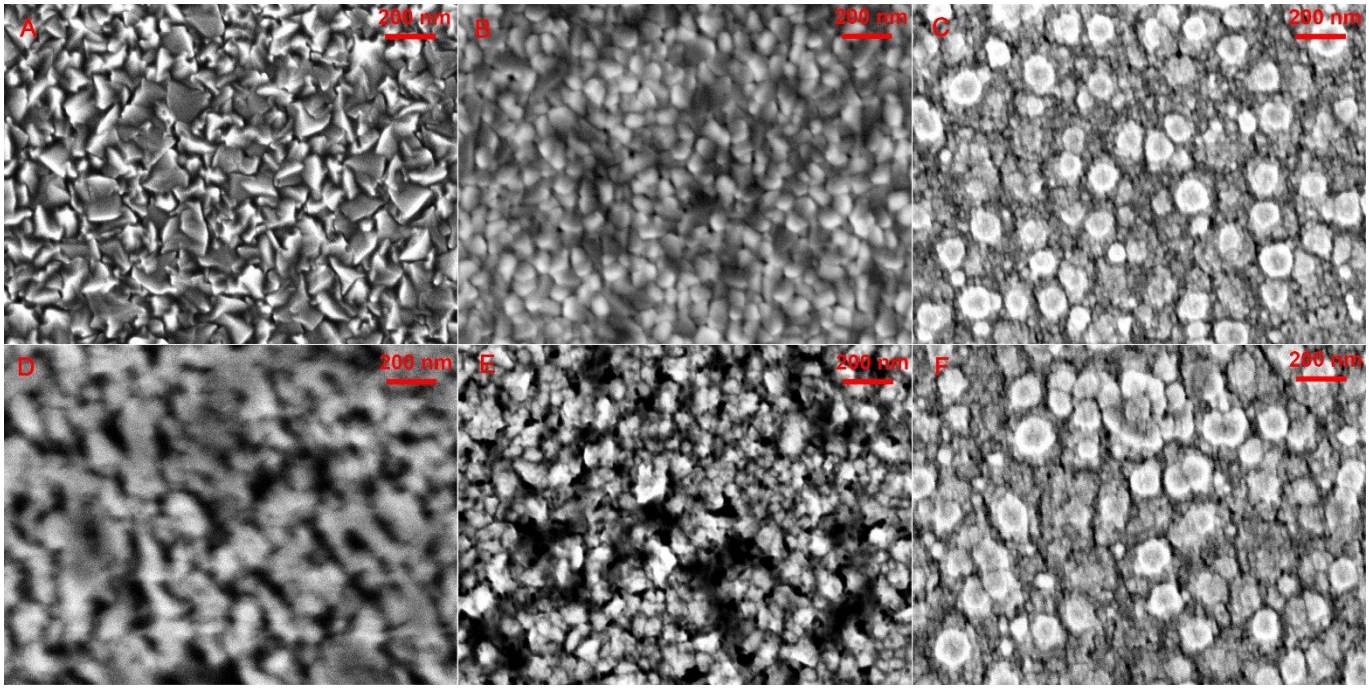

Figure S1. Top view SEM images of Cu_2O (A), Cu_2O/ZnO (B) and Cu_2O/ZnO/TiO_2 (C) before PEC water splitting. Top view SEM images of Cu_2O (D), Cu_2O/ZnO (E) and Cu_2O/ZnO/TiO_2 (F) after PEC water splitting.

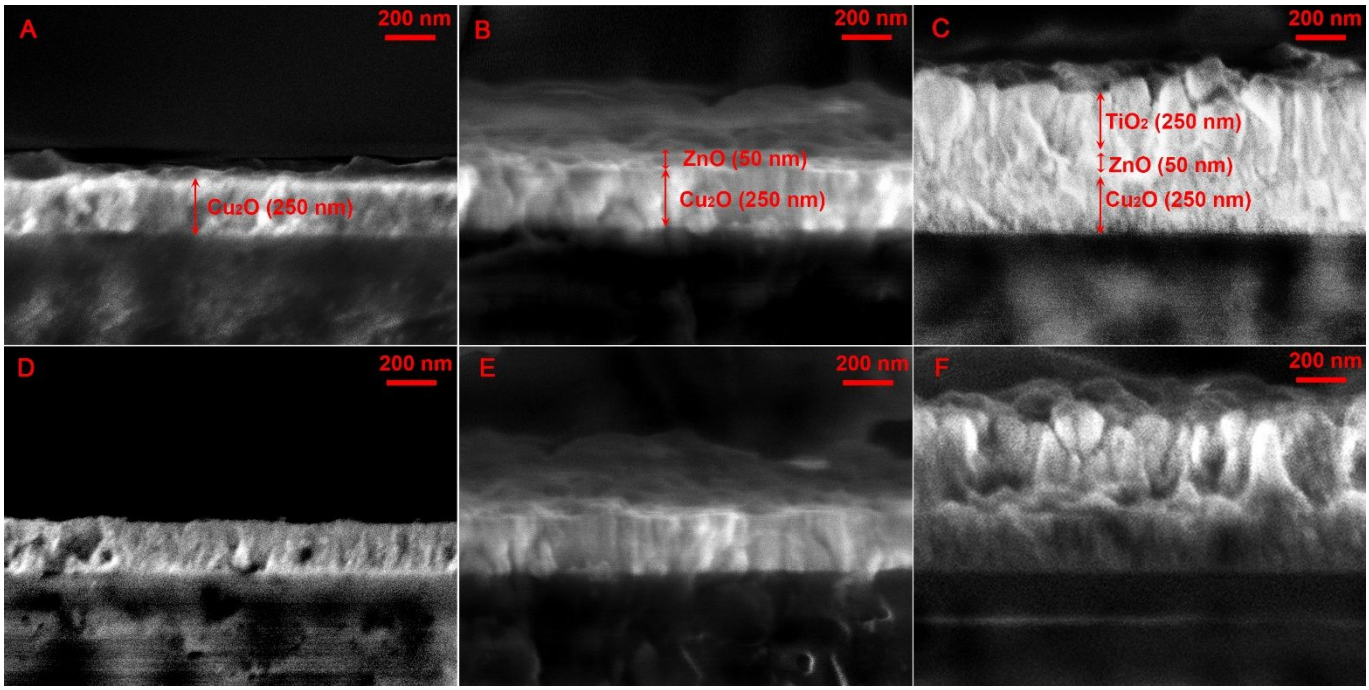

Figure S2. Cross-sectional SEM images of Cu_2O (A), Cu_2O/ZnO (B) and Cu_2O/ZnO/TiO_2 (C) before PEC water splitting. Cross-sectional SEM images of Cu_2O (D), Cu_2O/ZnO (E) and Cu_2O/ZnO/TiO_2 (F) after PEC water splitting.

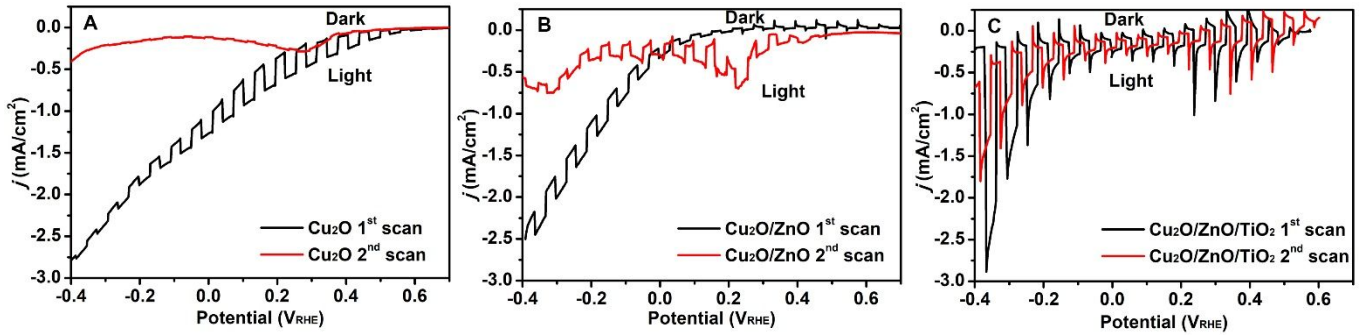

Figure S3. The *j-V* curves of Cu_2O (A), Cu_2O/ZnO (B) and Cu_2O/ZnO/TiO_2 (C) photocathodes for the 1st and 2nd scan. All the measurements were done in 0.1 M NaPi electrolyte solution (pH = 5) under chopped AM1.5G 100 mW/cm^2 illumination.

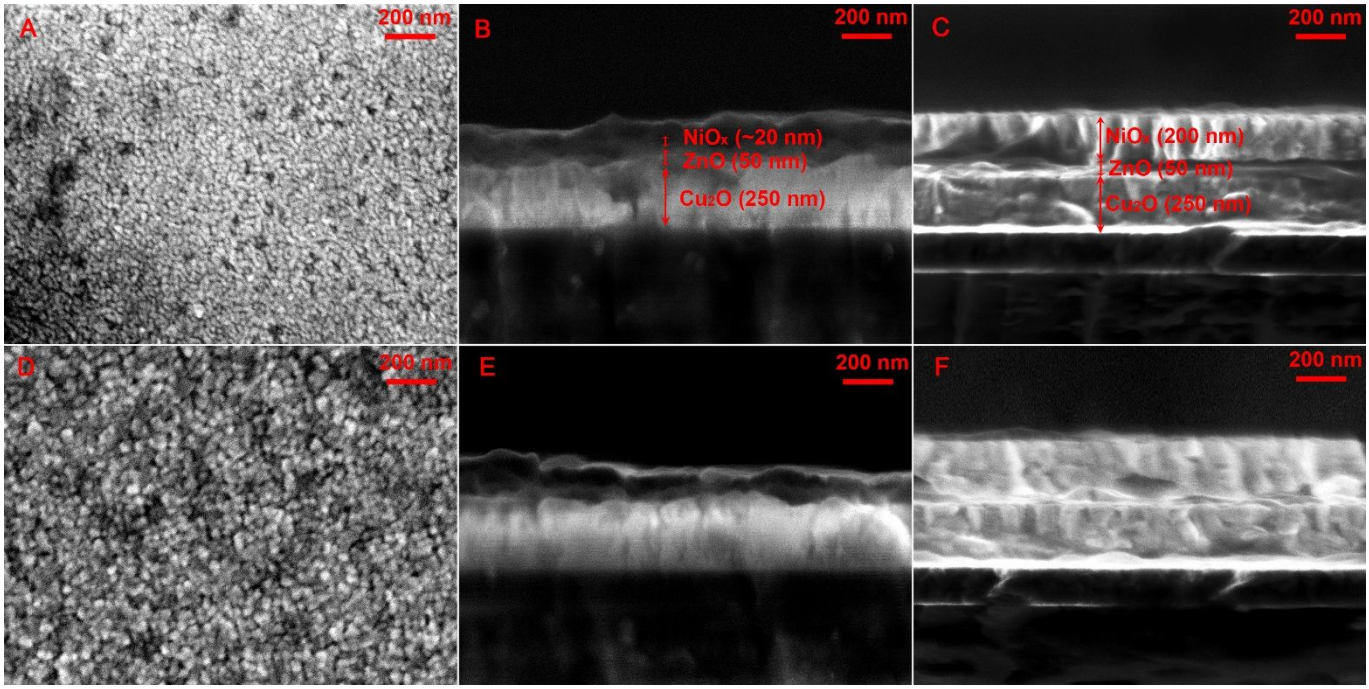

Figure S4. (A) Top view SEM image of Cu_2O/ZnO/NiO_x-200 nm before PEC water splitting. Cross-sectional SEM images of Cu_2O/ZnO/NiO_x-20nm (B) and Cu_2O/ZnO/NiO_x-200nm (C) before PEC water splitting. (D) Top view SEM image of Cu_2O/ZnO/NiO_x-200nm after PEC water splitting. Cross-sectional SEM images of Cu_2O/ZnO/NiO_x-20nm (E) and Cu_2O/ZnO/NiO_x-20nm (F) after PEC water splitting.

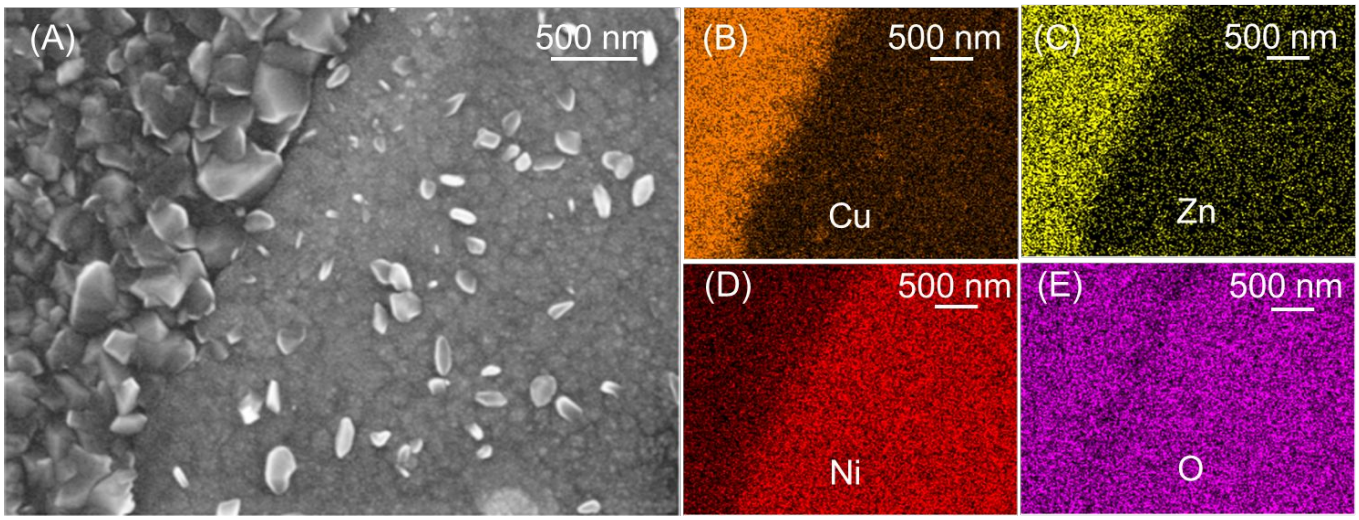

Figure S5. (A) Top view SEM image measured on the boundary between Cu_2O/ZnO region and the Cu_2O/ZnO/NiO_x-200nm region. Energy dispersive X-ray spectroscopy (EDXS) analysis of Cu (B), Zn (C), Ni (D) and O (E) elements on the boundary of Cu_2O/ZnO and Cu_2O/ZnO/NiO_x.

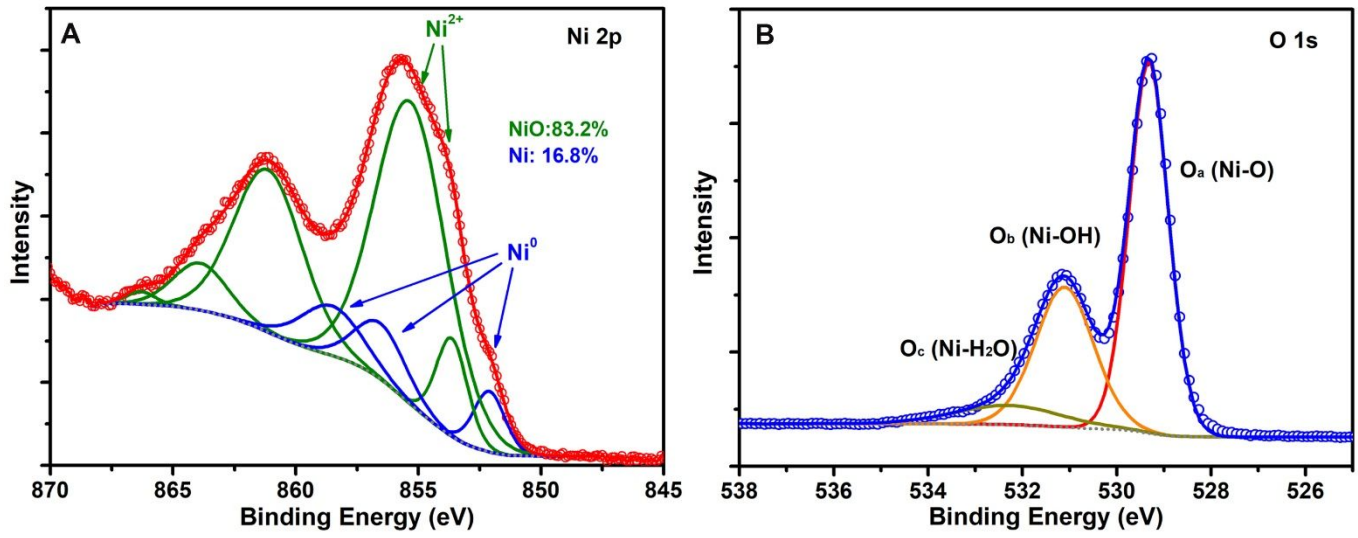

Figure S6. XPS spectra of the Ni 2p region (A) and the O 1s region (B) for the Cu_2O/ZnO/NiO_x-200nm sample.

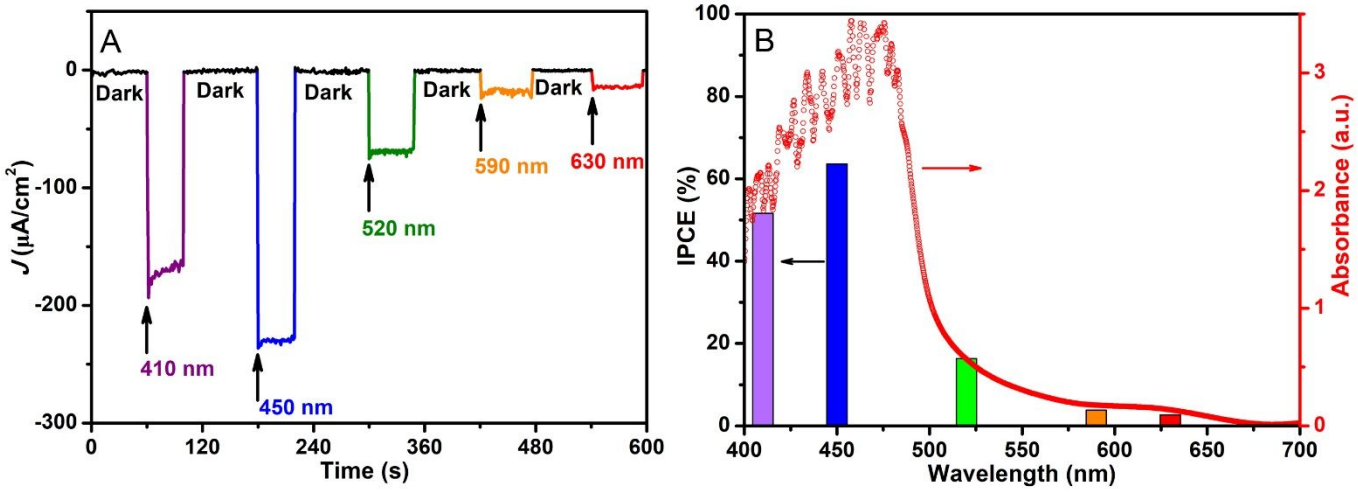

Figure S7. *J-t* curves (A) and IPCE (B) of the $Cu_2O/ZnO/NiO_x$-200nm photocathode measured in 0.1 M NaPi electrolyte solution (pH = 5.0) at 0 V_{RHE}. The different wavelength LEDs (line width of ~10 nm) with a light power of 1 mW/cm^2 were used as light sources.

Table S1. Cu_2O-based heterostructure photoelectrodes for PEC water splitting.

Photoelectrodes[a]	Fabrication methods	PEC measurements	Photocurrents (potential)[b]	References
FTO/Cu_2O/ZnO(21nm)/TiO_2(11nm)/Pt photocathode	Electrodeposition of Cu_2O; atomic layer deposition (ALD) of Al-doped ZnO; chemical deposition of TiO_2, electrodeposited of Pt	AM1.5G (100 mW/cm^2), 1.0 M Na_2SO_4 and 0.1 M KH_2PO_4 (pH 4.9)	-7.60 mA/cm^2 (0 V_{NHE})	A. Paracchino, et al, *Nat. Mater.*, **2011**, *10*, 456.[1] A. Paracchino, et al, *Energ. Environ. Sci.*, **2012**, *5*, 8673.[2]
Cu/nanoCu_2O/NiO_x(10 nm) photocathode	Chemical deposition of $Cu(OH)_2$, annealed at 500℃ for 1 h; spin-coating of $Ni(OAc)_2$, annealed at 200℃ for 30 min	White light (26 mW/cm^2), 0.1 M Na_2SO_4 solution (pH 6)	-4.98 mA/cm^2 (-0.33 V_{NHE})	C.-Y. Lin, et al, *Chem. Sci*, **2012**, *3*, 3482.[3]
ITO/Cu_2O/$SrTiO_3$(352 nm) photoanode	Spray pyrolysis deposition of $Cu(OAc)_2$; spin-coating of $Sr(OAc)_2$ and $Ti(OAc)_4$, annealed at 280℃	150 W Xe lamp (26 mW/cm^2), 0.1 M NaOH (pH 13)	2.52 mA/cm^2 (0.8 V_{SCE})	D. Sharma, et al, *J. Phys. Chem. C*, **2014**, *118*, 25320.[4]
FTO/Cu_2O/ZnO(20nm)/TiO_2(100nm)/RuO_2 photocathode	Electrodeposition of Cu_2O; ALD of Al-doped ZnO; chemical deposition of TiO_2, electrodeposited of RuO_2	AM1.5G (100 mW/cm^2), 0.5 M Na_2SO_4 and 0.1 M KH_2PO_4 (pH 5.0)	-5.5 mA/cm^2 (0 V_{NHE})	P. Dias, et al, *Adv. Energy Mater.*, **2015**, *5*, 1501537.[5]
FTO/Cu_2O/ZnO(20nm)/TiO_2(100nm)/RuO_2 photocathode	Sputter deposition of Cu, anodizing Cu to $Cu(OH)_2$, annealing at 600℃ for 4 h; ALD of Al-doped ZnO; chemical deposition of TiO_2, electrodeposition of RuO_2	AM1.5G (100 mW/cm^2), 0.5 M Na_2SO_4 and 0.1 M KH_2PO_4 (pH 5.0)	-10 mA/cm^2 (-0.3 V_{NHE})	J. S. Luo, et al, *Nano Lett*, **2016**, *16*, 1848.[6]
FTO/Cu_2O/NiO_x (240 nm) photocathode	Electrodeposited of Cu_2O; spin-coating of $Ni(OAc)_2$, annealed at 200℃	Visible light (100 mW/cm^2), 3M NaAc (pH 9-11), microbial anode in NaAc (pH 7)	159.7 μA/cm^2 (-0.1 V_{NHE})	D. Liang, et al, *Appl. Energy*, **2016**, *168*, 544.[7]
ITO/CeO_2(102nm)/Cu_2O photoanode	Spin-coating of $CeCl_3$, annealed at 500℃ for 5 h; spray pyrolysis deposition of $Cu(OAc)_2$	150 W Xe lamp (26 mW/cm^2), 0.1 M NaOH (pH 13)	2.89 mA/cm^2 (0.7 V_{SCE})	D. Sharma, et al, *Int. J. Hydrog. Energy*, **2016**, *41*, 18339.[8]
Cu mesh/Cu_2O photocathode	Chemical deposition of Cu_2O	AM1.5G (100 mW/cm^2), 0.1 M Na_2SO_4 (pH 7)	-4.80 mA/cm^2 (0 V_{RHE})	Z. X. Jin, et al, *J. Mater. Chem. A*, **2016**, *4*, 13736.[9]
FTO/NiO/Cu_2O/ZnO/TiO_2/Pt photocathode	Spin-coating of $Ni(OAc)_2$, annealed at 500℃ for 1 h; electrodeposition of Cu_2O; ALD of Al-doped ZnO; hydrothermal deposition of TiO_2; electrodeposition of Pt	AM1.5G (100 mW/cm^2), 0.5 M Na_2SO_4 and 0.1 M KH_2PO_4 (pH 4.15)	-2.74 mA/cm^2 (0 V_{RHE})	Y. Wei, X. Chang, T. Wang, C. Li, J. Gong, *Small*, **2017**, *13*, 1702007.[10]
FTO/WO_3 NRs/Cu_2O photoanode	Hydrothermal deposition of WO_3 at 180 ◦C for 24 h; electrodeposition of Cu_2O	AM1.5G (100 mW/cm^2), 1 M H_2SO_4 (pH 0)	1.37 mA/cm^2 (0.8 V_{RHE})	J. Zhang, et al, *Appl. Catal. B*, **2017**, *201*, 84.[11]
FTO/Cu_2O/g-C_3N_4 photoanode	Electrodeposition of Cu_2O; electrodeposition of g-C_3N_4	Xe lamp (≥ 400nm, 100 mW/cm^2), 0.1 M $NaNO_3$	-1.32 mA/cm^2 (-0.4 $V_{Ag/AgCl}$)	S. Zhang, et al, *Chinese J. Catal.*, **2017**, *38*, 365.[12]

Cu/p-Cu_2O/n-Cu_2O/ZnO/TiO_2/Pt photoanode	Electrodeposition of p- and n-type Cu_2O; ADL of Al-doped ZnO; hydrothermal deposition of TiO_2; electrodeposition of Pt	AM1.5G (100 mW/cm^2), 0.5 M Na_2SO_4 and 0.1 M KH_2PO_4 (pH 4.15)	-4.30 mA/cm^2 (0 V_{RHE})	T. Wang, et al, *Appl. Catal. B*, **2018**, *226*, 31.[13]
FTO/Cu_2O/ZnO (20nm) photocathode	Sputter deposition of Cu_2O, annealed at 550℃; ALD of Al-doped ZnO	AM1.5G (500 mW/cm^2), 0.5 M Na_2SO_4 and 0.1 M KH_2PO_4 (pH 4.15)	-7.23 mA/cm^2 (0 V_{RHE})	W. Z. Tawfik, et al, *J. Catal.*, **2019**, *374*, 276.[14]
FTO/ Cu_2O/NiO_x photocathode	Electrodeposition of Cu_2O; electrodeposition of $Ni(OH)_2$, annealed at 550℃ for 1 h	AM1.5G (100 mW/cm^2), 0.5 M Na_2SO_4 (pH 6)	-1.02 mA/cm^2 (0 V_{RHE})	H. L. S. Santos, et al, *J. Solid State Electrochem.*, **2020**, *24*, 1899.[15]
ITO/Cu_2O/ZnO (50nm)/NiO_x (200nm) photocathode	Sputter deposition of Cu_2O; sputter deposition of Al-doped ZnO; vacuum evaporation deposition of Ni, annealed at 400 °C	AM1.5G (100 mW/cm^2); 0.1 M NaH_2PO_4 (pH 5)	-0.84 mA/cm^2 (0 V_{RHE})	This work

Note: [a]Fluorine-doped tin oxide (FTO) coated glass, indium tin oxide (ITO) coated glass or Cu foil was used as substrate. [b]applied potential units of V_{NHE}, the potential *vs.* the normal hydrogen electrode; V_{SCE}, the potential *vs.* the saturated calomel electrode; $V_{Ag/AgCl}$, the potential *vs.* the Ag/AgCl electrode.

Table S2. Fitting results of EIS data for the Cu_2O, Cu_2O/ZnO, Cu_2O/ZnO/TiO_2-250nm and Cu_2O/ZnO/NiO_x-200nm photocathodes measured at 0 V_{RHE} under AM1.5G 100 mW/cm^2 illumination, as shown in Figure 4.

	Cu_2O	Cu_2O/ZnO	Cu_2O/ZnO/TiO_2	Cu_2O/ZnO/NiO_x
R_S (Ω cm^2)	0.2	0.1	0.1	0.1
$R_{ct,1}$ (Ω cm^2)	700	520	100	90
CPE_1-T	1.05×10^{-5}	1.05×10^{-5}	1.49×10^{-5}	1.05×10^{-5}
CPE_1-P	0.74	0.81	1	0.98
$R_{ct,2}$ (Ω cm^2)			2200	400
CPE_2-T			6.09×10^{-5}	8.00×10^{-5}
CPE_2-P			0.74	0.71

References:

(1) Paracchino, A., Laporte, V., Sivula, K., Grätzel, M. and Thimsen, E., Highly Active Oxide Photocathode for Photoelectrochemical Water Reduction, *Nat. Mater.*, **2011**, *10*, 456.

(2) Paracchino, A., Mathews, N., Hisatomi, T., Stefik, M., Tilley, S. D. and Grätzel, M., Ultrathin Films on Copper(i) Oxide Water Splitting Photocathodes: a Study on Performance and Stability, *Energ. Environ. Sci.*, **2012**, *5*, 8673-8681.

(3) Lin, C.-Y., Lai, Y.-H., Mersch, D. and Reisner, E., $Cu_2O|NiO_x$ Nanocomposite as an Inexpensive Photocathode in Photoelectrochemical Water Splitting, *Chem. Sci.*, **2012**, *3*, 3482-3487.

(4) Sharma, D., Upadhyay, S., Satsangi, V. R., Shrivastav, R., Waghmare, U. V. and Dass, S., Improved Photoelectrochemical Water Splitting Performance of $Cu_2O/SrTiO_3$ Heterojunction Photoelectrode, *J. Phys. Chem. C*, **2014**, *118*, 25320-25329.

(5) Dias, P., Schreier, M., Tilley, S. D., Luo, J. S., Azevedo, J., Andrade, L., Bi, D. Q., Hagfeldt, A., Mendes, A., Gratzel, M. and Mayer, M. T., Transparent Cuprous Oxide Photocathode Enabling a Stacked Tandem Cell for Unbiased Water Splitting, *Adv. Energy Mater.*, **2015**, *5*, 1501537.

(6) Luo, J. S., Steier, L., Son, M. K., Schreier, M., Mayer, M. T. and Gratzel, M., Cu_2O Nanowire Photocathodes for Efficient and Durable Solar Water Splitting, *Nano Lett*, **2016**, *16*, 1848-1857.

(7) Liang, D., Han, G., Zhang, Y., Rao, S., Lu, S., Wang, H. and Xiang, Y., Efficient H_2 Production in a Microbial Photoelectrochemical Cell with a Composite Cu_2O/NiO_x Photocathode under Visible Light, *Appl. Energy*, **2016**, *168*, 544-549.

(8) Sharma, D., Satsangi, V. R., Shrivastav, R., Waghmare, U. V. and Dass, S., Understanding the Photoelectrochemical Properties of Nanostructured CeO_2/Cu_2O Heterojunction Photoanode for Efficient Photoelectrochemical Water Splitting, *Int. J. Hydrog. Energy*, **2016**, *41*, 18339-18350.

(9) Jin, Z. X., Hu, Z. F., Yu, J. C. and Wang, J. F., Room Temperature Synthesis of a Highly Active Cu/Cu_2O Photocathode for Photoelectrochemical Water Splitting, *J. Mater. Chem. A*, **2016**, *4*, 13736-13741.

(10) Wei, Y., Chang, X., Wang, T., Li, C. and Gong, J., A Low-Cost NiO Hole Transfer Layer for Ohmic Back Contact to Cu_2O for Photoelectrochemical Water Splitting, *Small*, **2017**, *13*, 1702007.

(11) Zhang, J., Ma, H. and Liu, Z., Highly Efficient Photocatalyst Based on all Oxides WO_3/Cu_2O Heterojunction for Photoelectrochemical Water Splitting, *Appl. Catal. B*, **2017**, *201*, 84-91.

(12) Zhang, S., Yan, J., Yang, S., Xu, Y., Cai, X., Li, X., Zhang, X., Peng, F. and Fang, Y., Electrodeposition of $Cu_2O/g\text{-}C_3N_4$ Heterojunction Film on an FTO Substrate for Enhancing Visible Light Photoelectrochemical Water Splitting, *Chinese J. Catal.*, **2017**, *38*, 365-371.

(13) Wang, T., Wei, Y., Chang, X., Li, C., Li, A., Liu, S., Zhang, J. and Gong, J., Homogeneous Cu_2O p-n Junction Photocathodes for Solar Water Splitting, *Appl. Catal. B*, **2018**, *226*, 31-37.

(14) Tawfik, W. Z., Hassan, M. A., Johar, M. A., Ryu, S.-W. and Lee, J. K., Highly Conversion Efficiency of Solar Water Splitting over p-Cu_2O/ZnO Photocatalyst Grown on a Metallic Substrate, *J. Catal.*, **2019**, *374*, 276-283.

(15) Santos, H. L. S., Corradini, P. G., Andrade, M. A. S. and Mascaro, L. H., CuO/NiO_x Thin Film-Based Photocathodes for Photoelectrochemical Water Splitting, *J. Solid State Electrochem.*, **2020**, *24*, 1899-1908.